Lawrence Berkeley National Laboratory
LBL Publications

Title
UV Photodissociation of Furan Probed by Tunable Synchrotron Radiation

Permalink
https://escholarship.org/uc/item/4dx8t8n7

Authors
Sorkhabi, Osman
Qi, Fei
Rizvi, Abbas H
et al.

Publication Date
1999-02-01

ERNEST ORLANDO LAWRENCE BERKELEY NATIONAL LABORATORY

UV Photodissociation of Furan Probed by Tunable Synchrotron Radiation

Osman Sorkhabi, Fei Qi, Abbas H. Rizvi,
and Arthur G. Suits

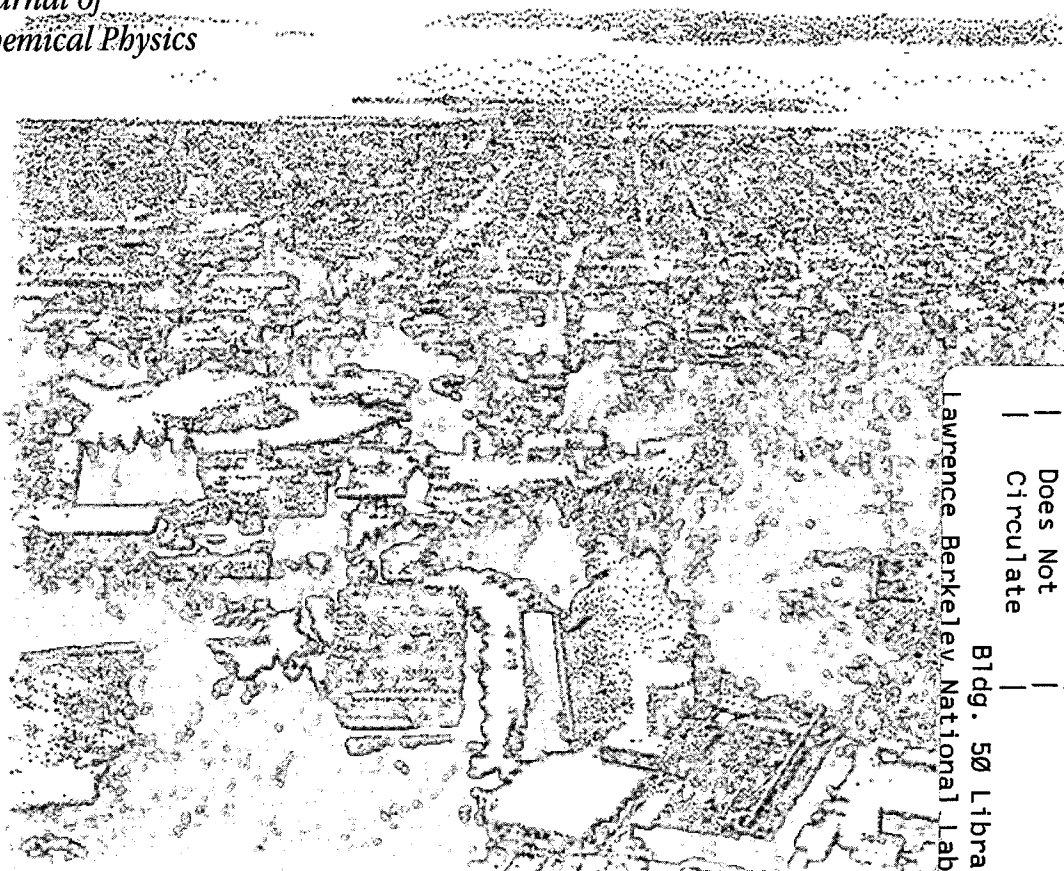**Chemical Sciences Division**

DISCLAIMER

UV Photodissociation of Furan Probed by Tunable Synchrotron Radiation

Osman Sorkhabi, Fei Qi, Abbas H. Rizvi, and Arthur G. Suits

Chemical Sciences Division
Ernest Orlando Lawrence Berkeley National Laboratory
University of California
Berkeley, California 94720

February 1999

UV Photodissociation Of Furan Probed by Tunable Synchrotron Radiation

Osman Sorkhabi, Fei Qi, Abbas H. Rizvi, and Arthur G. Suits

Chemical Sciences Division, Lawrence Berkeley National Laboratory, Berkeley, CA 94720

Abstract

The photodissociation dynamics of furan at 193 nm have been studied using photofragment translational spectroscopy with tunable VUV probe provided by synchrotron radiation on the Chemical Dynamics Beamline at the Advanced Light Source. Three primary channels are observed: $HCO+C_3H_3$, $CO+C_3H_4$ and $H_2CCO + C_2H_2$. The evidence suggests that the two closed shell channels occur on the ground state potential energy surface (PES) following internal conversion, while the radical channel likely takes place on an excited PES. All channels exhibit a barrier for dissociation with the acetylene + ketene channel having the largest value at about 25 kcal/mol. Angular distribution measurements show anisotropy only for the radical channel. These findings are consistent with a rapid excited state dissociation for the radical channel and slow dissociation for the other two pathways. The two ground state dissociation channels - propyne + CO and acetylene + ketene - should be important in the thermal decomposition of furan as was found in pyrolytic studies [A. Lifshitz, M. Bidani, and S. Bidani, *J. Phys. Chem.*, **90**, 5373 (1986)] and theoretical investigations [R. Liu, X. Zhou, and L. Zhai, *J. Comput. Chem.*, **19**, 240 (1998)].
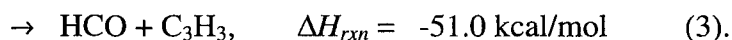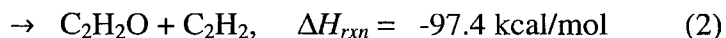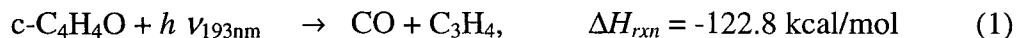
INTRODUCTION

Unimolecular dissociation pathways of cyclic molecules play an important role in the combustion of organic matter.[1] It is believed that chemical pathways leading to the destruction and formation of cyclic molecules determine the fate of combustion by-products such as polycyclic aromatic hydrocarbons (PAHs) and in soot formation.[1,2] Unimolecular dissociation (or thermal decomposition) of molecules in combustion processes occurs as a result of the elevated temperatures, and dissociation proceeds mostly on the ground state potential energy surface (PES). Pyrolytic studies of cyclic compounds has yielded useful information on the thermal decomposition of many cyclic molecules.[3-7] These studies are, however, complicated by the presence of multiple secondary reactions and rigorous computer modeling must be done to determine the primary processes.[3] Photochemical studies in molecular beams, on the other hand, can provide unambiguous information on the primary processes following unimolecular dissociation.

In this paper, we will present results for the ultraviolet photodissociation of furan obtained on the Chemical Dynamics Beamline at the Advanced Light Source. The unique combination of photofragment translational spectroscopy with intense, tunable undulator radiation available on the Beamline allows for detailed investigation of complex polyatomic dissociation dynamics, as has been shown for a number of systems[8]. Ultraviolet excitation of polyatomic molecules is often rapidly followed by internal conversion to the ground state potential surface. When the corresponding dynamics are clearly distinct from those involving excited electronic states, one may study ground state dissociation dynamics under collision free conditions and at well-defined energies. Furthermore, excited state dissociation dynamics can also be studied to yield information about the nature of the excited state PES's.

Furan and other oxygen containing cyclic molecules are expected to be important combustion intermediates due the heavy use of oxygenated fuel additives in gasoline in recent years.[9] No literature exits on the photochemistry of furan. A pyrolytic investigation was carried out by Lifshitz, *et al.*, however.[7] Propyne, acetylene, and carbon monoxide were found to be the major decomposition products. In a recent

theoretical treatment, Liu *et al.* confirmed these findings.[10] The results of Liu *et al.* implied that the formation of propyne + CO proceeded via the lowest energy pathway in the unimolecular dissociation of furan - a finding consistent with the experimental results of Lifshitz. Acetylene and ketene were suggested to be minor products. Our results indicate the presence of three primary channels:

$$c\text{-}C_4H_4O + h\nu_{193nm} \rightarrow CO + C_3H_4, \qquad \Delta H_{rxn} = -122.8 \text{ kcal/mol} \qquad (1)$$

$$\rightarrow C_2H_2O + C_2H_2, \quad \Delta H_{rxn} = -97.4 \text{ kcal/mol} \qquad (2)$$

$$\rightarrow HCO + C_3H_3, \quad \Delta H_{rxn} = -51.0 \text{ kcal/mol} \qquad (3).$$

Evidence will be presented indicating that reactions (1) and (2) occur on the ground state PES following internal conversion. Reaction (3) was not observed in the unimolecular dissociation studies.

EXPERIMENTAL

All experiments were conducted at beamline 9.0.2.1 of the Advanced Light Source using a rotatable source molecular beam machine which has been described in detail elsewhere.[11] Helium was bubbled through a furan sample held at –21 °C. At this temperature and a total pressure of 800 Torr, a 10% molecular beam of furan/He was generated. This mixture was fed through pulsed valve (General Valve) and expanded from a nozzle heated to ~100°C in a differentially pumped source region and into the main chamber. The pressure in the source chamber was maintained at 2×10^{-4} Torr with the beam on. The molecular beam was collimated with two skimmers (0.03" and 0.02") and its velocity and speed ratio were either measured by using a chopper wheel or a laser hole-burning method. Both methods gave consistent results and typical values for the velocity and speed ratio were found to be 1400 ± 50 m s^{-1} and 9 ± 1, respectively.

The photolysis laser was an ArF excimer (193.3 nm, Lambda Physik LPX 220i), focused to a spot of size 2x4 mm and aligned perpendicular to the plane containing the molecular beam and detector axis, on the axis of rotation of the molecular beam source. Photofragments entering the triply differentially pumped detector region (9×10^{-11} Torr) were photoionized 15.2 cm from the interaction region using tunable synchrotron radiation. The characteristics of the light source are discussed in detail elsewhere, but include an intensity of 10^{16} photons/sec (quasi-continuous), an energy bandwidth of

2.2%, and a cross section in the probe region of 0.2x0.1 mm. The tunability of the light source allows for selective ionization of products and very low background counts. The photoionized products were mass selected by using a quadrupole mass filter and the ions were counted with a Daly ion counter.[12] Time-of-flight of the products were measured with a multichannel scalar (EG&G Ortec Turbo MCS). The bin width for the MCS was fixed at 0.75 or 1 μsec for the measurements reported here. Timing sequences for the laser, pulsed valve, and the MCS were maintained by a digital delay generator (Stanford Research Systems, Inc. Model 535). Ten quartz plates fixed at Brewster's angle were used for the polarization measurements to give 87±5% polarized light. To rotate the angle of polarization with respect to the detector axis, a half wave plate was used (Karl Lambrecht). Furan (99%) was obtained from Aldrich and used without further purification.

RESULTS

Using the enthalpies of reactions for the observed primary processes, the measured beam velocity, and the masses of the fragments, one can calculate the energetic limit for the spatial distribution of all the observed fragments, summarized in the 'Newton' diagram in Fig. 1. Notice from Fig. 1 that every fragment may be scattered over all laboratory angles with respect to the molecular beam axis. Measurements for all of the fragments were taken at multiple angles to ensure the reliability of the forward convolution fits to the data.[13] Care was taken to ensure that each channel was a one-photon event. This was achieved by measuring the signal as a function of laser intensity and recording data when this relationship was linear. Comparisons were also made between TOF spectra measured with different laser intensities to confirm that single photon events were being observed. Signal was observed for m/e 26, 28, 29, 39, 40, and 42. These masses correspond to C_2H_2, CO, HCO, C_3H_3, C_3H_4, and C_2H_2O photofragments, respectively.

The radical channel

The strongest signals were observed at m/e 39 ($C_3H_3^+$). Time-of-flight (TOF) data at both 20° and 50° are plotted in Fig 2. This data was fitted with the P(E) shown in

Fig. 3. Note that the P(E) peaks slightly away from zero and extends out to about 35 kcal/mol, with an average energy release of 11.3 kcal/mol. The fit to the data is reasonably good. However, when attempts were made to fit the counter fragment, m/e 29 (HCO^+), also shown in Fig. 2, only the low energy portion of the m/e 39 distribution was found to make a contribution to the m/e 29 signal. The P(E) used to fit the m/e 29 data is shown as the dashed line in Fig. 3. As discussed below, this is consistent with what is expected given the weak bond in HCO (20.8 kcal/mol), giving rise to secondary decomposition of the bulk of the primary HCO product. Indeed, a large contribution to the m/e 28 signal arises directly from this process, and is momentum-matched to the m/e 39 data.

One of the advantages of using the tunable VUV to photoionize the products (as opposed to the use of electron impact ionization, for example) is that it allows for the selective ionization of the different fragments. One can therefore establish the identity of a certain mass fragment by measuring its photoion yield signal. Fig. 4 shows the photoion yield spectra for m/e 29 and 39, with published values for the ionization onset for the HCO and propargyl radicals (H_2CCCH) indicated by the arrows. From this data, we conclude that the most likely identity of the m/e 39 product is the lowest energy propargyl isomer, H_2CCCH.

The CO + C_3H_4 channel

For m/e 28, CO, the momentum-matched partner is m/e 40, C_3H_4. Both of these fragments show large contributions from the dominant radical channel as discussed below. Measured TOF spectra for these two masses at 20° and 50° are shown in Fig. 5, along with forward convolution fits to the data obtained using the P(E) shown in Fig. 6. Figure 7 shows the photoionization yield spectrum for m/e 40. The identity of m/e 40 product is more challenging to establish since the two likely isomers of C_3H_4 – propyne and allene – have similar ionization potentials, 10.36 eV and 9.69 eV, respectively. There appear to be two ionization onsets in the photoion yield spectrum in Fig. 7, one at 8.75 eV and another at 10.25 eV. The ionization onset at 8.75 eV is identical to that shown above for m/e 39, the propargyl radical. The signal for m/e 39 is about 100 times larger than that for m/e 40, so that a small contribution resulting from mass leakage in the

quadrupole from m/e 39 to the m/e 40 signal is responsible for the observation of two onsets. By scaling the m/e 39 contribution at the obvious break that appears in both spectra, we can subtract this contribution to obtain the photoion yield for the m/e 40 contribution alone, shown by the dashed line in Fig. 7. The corrected signal for m/e 40 shows an onset of 9.5 eV. This is near the threshold for allene; however, as these are largely vibrationally excited products, we anticipate a significant red-shift in the ionization onset. As a result, it is most likely due to propyne, consistent with the findings of Liu, *et al.* whose calculations indicated that ground state unimolecular dissociation of furan to CO + propyne followed a path 23 kcal/mol lower in energy than the path leading to CO + allene.[10]

The $P(E)$ shown in Fig. 6 was used to fit the CO + C_3H_4 channel. The P(E) peaks at 12 kcal/mol, extends to 44 kcal/mol and shows an average energy release of 16.7 kcal/mol. The m/e 40 data also includes a contribution from the much larger m/e 39 signal, consistent with the photoion yield spectra above, fitted with the corresponding P(E) from Fig. 3. The CO was then fitted with contributions that are strictly momentum-matched to the m/e 40 P(E) (Fig. 6) and the HCO secondary decomposition as discussed above. The necessary consistency of all these fits along with the photoion yield spectra provide an important check on the analysis, and show the importance of the tunable VUV photoionization to aid in unraveling these complex decomposition processes.

C_2H_2 + *ketene channel*

The TOF spectra for the momentum-matched fragments m/e 26 and m/e 42 at 20° and 50° are plotted in Fig. 8. These masses correspond to acetylene (C_2H_2) and ketene (H_2CCO), respectively. These were fitted with the P(E) shown in Fig. 9. This P(E) peaks at about 25 kcal/mol, extends to 60 kcal/mol and shows an average energy release of 26.7 kcal/mol. The peak location indicates the presence of a barrier of at least 25 kcal/mol for this process [i.e. reaction (2)], is in reasonable agreement with the calculated value of 35 kcal/mol[10] and the experimentally derived value of 33 kcal/mol[7] for the ground state unimolecular dissociation of furan to acetylene and ketene. A larger fraction of the available energy goes into the translational degrees of freedom of the products as

compared to reaction (1). We will comment more on this in the discussion section below. For m/e 26 ($C_2H_2^+$), a contribution arising from secondary decomposition of C_3H_4 to give $C_2H_2 + CH_2$ gives rise to very slow peak as seen in Fig. 8. This small contribution is exaggerated by the experimental sensitivity to products that have a near-zero center of mass recoil velocity.

Angular Distribution Measurements

From the P(E) curves, the largest translational energy release occurs for the ketene + acetylene channel [reaction (2)] followed by CO + propyne [reaction (1)] and HCO + propargyl radical [reaction (3)], respectively. In addition to the translational energy distributions, the signal for m/e 26, 28, and 39 were measured as a function of laser polarization angle. This data is plotted in Fig. 10 and was fitted according to $P(\theta) = 1 + \beta P_2(\cos(\theta - \gamma))$ where γ is the lab-to-CM offset angle and β is the well-known anisotropy parameter.[14] For m/e 39, the best fit to the data yielded a value of -0.2 for β while β was found to be nearly zero for m/e 26 and 28.

DISCUSSION

The radical channel

Several aspects of the dynamics for this process indicate that the radical channel is distinct, and likely occurs directly on an electronically excited PES. First, this channel (reaction 3) has not been observed in the unimolecular dissociation of furan, and indeed lies at much higher energy than the ground state barrier to the CO + propyne channel, for example (see the energy diagram in Fig. 11). Second, an anisotropic angular distribution was observed for this channel, clearly indicating a prompt dissociation process. Finally, although it is difficult to be quantitative on the product branching owing to uncertainties in the photoionization efficiencies, this channel clearly dominates over the other, energetically favored processes. A possible mechanism for this channel may consist of ring opening (a C_5-O_1 bond cleavage) on the electronically excited state PES followed by a 4,3-hydride shift and a C_3-C_2 bond cleavage to give HCO + propargyl radical (C_3H_3). Although a concerted C_5-O_1 and C_2-C_3 bond cleavage could also lead to the same

7

products, this seems unlikely because of the small amount of energy that goes into product translation. In other words, the center of mass for such a geometry lies almost in the center of the ring and a concerted dissociation from that geometry would impart a large amount of translational energy on the recoiling fragments. Only 22% of the available energy goes into product translation implying that it is more likely for the ring to open before dissociation.

The average energy release in the HCO + propargyl channel is about 12 kcal/mol and the available energy for reaction (3) is 51 kcal/mol. Therefore, an average of 39 kcal/mol can be distributed into the internal energy of the products. This is enough energy to produce HCO in the metastable A $^2A''$ (Π) electronic state, which has a T_0 of 26.6 kcal/mol. However, such a process would require that the C_3H_3 fragment be internally 'cold'. The photoion yield spectrum (Fig. 4) for C_3H_3 indeed indicates that this fragment has little internal energy. In addition, it is curious that the HCO that appears to survive without decomposition is the *slowest* HCO product, normally corresponding to those with the greatest internal energy. One possible explanation for this anomaly would be that the slower HCO products represent the production of electronically excited HCO molecules that fluoresce to produce cold ground state HCO. Additional studies (e.g. looking for chemiluminsescence) would be necessary to confirm this suggestion.

As mentioned above, anisotropy measurements for this channel produced a beta parameter of –0.2. Measurement of a negative β indicates that the transition dipole has a component perpendicular to the dissociation coordinate. Excitation of the $1a_2 \rightarrow 3p$ Rydberg series of furan at 193 nm has a transition moment aligned across the π systems (with the upper state being $^1B_2$ under the C_{2v} point group).[15] Therefore, decomposition of the molecule on a line along the C_{2v} axis should lead to a negative beta parameter. The slightly negative value for the β parameter is consistent with recoil at some modest angle to the C_{2v} axis. Furthermore, the nonzero β indicates that dissociation occurs on a rapid time scale relative to the rotational period. The ring opening, the 4,3-hydride shift, and the C_2-C_3 bond cleavage must, therefore, occur rapidly.

A comparison with the UV photodissociation study of thiophene, the sulfur-containing analog of furan, shows interesting similarities with this channel.[16] The 193

8

nm dissociation of thiophene yielding the following channel is analogous to reaction (3): $C_4H_4S + h\nu \rightarrow C_3H_3 + HCS$. The $P(E)$ for this channel was found to peak at zero and extend to 15 kcal/mol indicating that little energy is released into product translation: a finding very similar to that found for reaction (3).

$CO + C_3H_4$ channel

Reaction (1) likely occurs on the ground state PES since it has been observed in the unimolecular shock tube experiment of Lifshtz, et al.[7] and later verified by the calculations of Liu, et al.[10] Therefore, prompt internal conversion (IC) must follow the initial excitation by the 193 nm laser pulse. The following mechanism for this channel was postulated by Liu and co-workers; a 4,5-hydride shift followed by ring opening and subsequent dissociation to give CO + propyne.[10] Liu, et al. also calculated an energy profile for this mechanism and found an activation energy of 77 kcal/mol for reaction (1) at the QCISD(T) / 6-311++G** level of theory (see Fig. 11). The channel leading to CO + allene was found to have an activation energy of 100 kcal/mol. Therefore, the CO + propyne channel should be the most probable one. The photon energy at 193nm is 148 kcal/mol, so that ground state furan after IC lies well above the barriers to dissociation for all possible channels. Assuming an RRKM type process for the dissociation, the CO + propyne channel will clearly dominate. Our photoion yield measurements for m/e C_3H_4 indicates that the observed signal for this mass, after accounting for the C_3H_3 contamination, is due primarily to propyne – which is consistent with the theoretical measurements of Liu et al.;[10] the experimental results of Lifshtz and co-workers;[7] and the above analysis.

Angular distribution measurements for this channel yielded an isotropic product distribution (i.e. $\beta = 0$). This implies the dissociation process takes place on a time scale longer than several molecular rotation periods. The P(E) for this reaction indicates that 17% of the available energy goes into product translational energy. CO and C_3H_4 should therefore have very 'hot' internal energy distributions. This is consistent with a slow dissociation in which the available energy is randomized within the degrees of freedom of the molecule before dissociation takes place. Fig. 12 shows that even below the ionization threshold for CO, strong signal is observed for m/e 28, although the faster,

9

colder product is discriminated against. This is evidence of vibrational excitation in the CO . In fact, CO can be excited at least up to $v = 2$ according to Fig. 12

Another reported dissociation channel of thiophene at 193 nm $C_3H_4 + CS$.[16] This channel bears striking resemblance to reaction (1). The P(E) was found to peak at about 10 kcal/mol and extended to 30 kcal/mol. Although the energetics for this process are different, the $P(E)$ is similar to the one for reaction (1). Work is in progress in our laboratory to obtain a detailed set of data for the photodissociation of thiophene at 193 nm.

C_2H_2 + ketene channel

A mechanism, proposed by Liu $et\ al.$, for reaction (2) consisted of a 5,4-hydride shift followed by a concerted C_3-C_4 and O_1-C_2 bond cleavage to give $C_2H_2O + C_2H_2$.[10] The 5,4-hydride shift was found to leave the geometry of the ring undisturbed and the center-of-mass for a concerted dissociation from such a geometry lies almost in the center of the ring. Such a mechanism should lead to translationally excited products. Fig. 7 shows the center-of-mass translational energy distribution for reaction (2). This P(E) indicates the presence of a barrier of at least 25 kcal/mol for this process. The energy profile for this mechanism was calculated by Liu and co-workers and the activation energy was found to be 80 kcal/mol with respect to ground state furan.[10] This corresponds to a reaction barrier of 35 kcal/mol with respect to products. The experimentally derived value for the activation energy was reported to be 77.5 kcal/mol and corresponds to a reaction barrier of 33 kcal/mol.[7] Both of these results are in good agreement with our finding of 25 kcal/mol for this value.

Anisotropy measurements yielded a beta parameter of nearly zero indicating an isotropic angular distribution. This finding also suggests that the dissociation process is not a rapid one and thus at least partial randomization of energy takes place prior to dissociation. As mentioned above, a larger fraction of the available energy (22%) goes into product translational energy; this likely reflects the presence of the large barrier.

A comparison with the dissociation of thiophene at 193 nm indicates many similarities for this channel as well. The 193 nm dissociation of thiophene yielding the following channel is analogous to reaction (2): $C_4H_4S + h\nu \rightarrow C_2H_2S + C_2H_2$. The

10

experimentally derived $P(E)$ for this channel was found to peak at ~18 kcal/mol and extended to 40 kcal/mol suggesting a reaction barrier of 18 kcal/mol for this process.[16] This reaction barrier is remarkably similar to the one we have derived for reaction (2), again implying that the mechanism for the UV dissociation dynamics of thiophene and furan are very similar. Both furan and thiophene are heterocyclic dienes and, thus, have similar electronic structure.[17] For furan, the transition at 193 nm belongs to the $1a_2 \rightarrow 3p$ Rydberg series and it appears that a similar transition is excited in thiophene. The dynamics is dominated by the electronic structure, even though the energetics and the relative masses of the fragments are different for the dissociation of furan and thiophene.

Conclusion

We have studied the dissociation dynamics of furan at 193 nm using photofragment translational spectroscopy with tunable VUV probe provided by intense synchrotron radiation. Three product channels are observed. Two of these result in closed shell molecular products and occur on the ground electronic surface following internal conversion. The results for these channels are consistent with recent theoretical studies and shock-tube results. The third channel gives rise to radical products and is shown to occur as a direct process on an electronically excited potential energy surface.

Acknowledgments

REFERENCES

1. I. Glassman, *Combustion*. 2nd Ed. Academic Press, New York (1987).

2. M. J. Castaldi and S. M. Senkan, *Combust. Sci. and Tech.*, **116-117**, 167 (1996) and references therein.

3. A. Lifshitz, C. Tamburu, and R. Shashua, *J. Phys. Chem.* A, **101**, 1018 (1997).

4. R. Liu, K. Morokuma, A. M. Mebel, and M. C. Lin, *J. Phys. Chem.*, **100**, 9314 (1996).

5. A. Laskin and A. Lifshitz, *J. Phys. Chem.* A, **102**, 928 (1997).

6. H. Wang and K. Brezinsky, *J. Phys. Chem.* A, **102**, 1530 (1998).

7. A. Lifshitz, M. Bidani, and S. Bidani, *J. Phys. Chem.*, **90**, 5373 (1986).

8. D.A. Blank, S.W. North, D. Stranges, A.G. Suits and Y.T. Lee, *J. Chem. Phys.*, **106**, 539 (1997); D. A. Blank, A. G. Suits, Y. T. Lee, S. W. North, G. W. Hall, *J. Chem. Phys.*, **108**, 5784 (1998); W. Sun, J. Robinson, K. Yokoyama, A. G. Suits and D. M. Neumark *J. Chem. Phys.* **110**, 4363 (1999).

9. K. Owen, *Gasoline and Diesel Fuel Additives*, John Wiley & Sons, New York (1989).

10. R. Liu, X. Zhou, and L. Zhai, *J. Comput. Chem.*, **19**, 240 (1998).

11. X. Yang, J. Lin, Y. T. Lee, D. A. Blank, A. G. Suits, and A. M. Wodke, *Rev. Sci. Instrum.*, **68**, 3317 (1997).

12. Y. T. Lee, J. D. McDonald, P. R. LeBreton, and D. R. Herschbach, *Rev. Sci. Instrum.*, **40**, 1402 (1969).

13. A. M. Wodke, Ph.D. Thesis, University of California, Berkeley (1986); X. Zhao, Ph.D. Thesis, University of California (1988).

14. R. N. Zare, *Mol. Photochem.*, **4**, 1 (1974).

15. M. H. Palmer, I. C. Walker, C. C. Ballard, and M. F. Guest, *Chem. Phys.*, **192**, 111 (1995).

16. J. D. Meyers, Ph.D. Thesis, University of California, Berkeley (1993).

17. M. B. Robin, *Higher Excited States of Polyatomic Molecules*, vol. II, pg. 180-189, Academic Press, New York (1975).

Figure Captions

1. Newton diagram for the experiment showing the recoil velocity limits for all products.

2. Time of flight spectra for the indicated mass and laboratory scattering angle. Circles are experimental points, the line is the result of the simulation.

3. Translational energy distribution obtained from the fit to the data in Fig. 2. Solid line is the result for the m/e = 39 data, the dashed line is for the m/e 29 data.

4. Photoionization efficiency curves for the indicated product at a laboratory scattering angle of 20°.

5. Time of flight spectra for the indicated mass and laboratory scattering angle. Circles are experimental points, the dashed line is the primary $CO+C_3H_4$ contribution, and the dot-dash line is the $HCO+C_3H_3$ contribution. The solid line is the full simulation.

6. Translational energy distribution obtained from the fit to the data in Fig. 5 for the $CO+C_3H_4$ channel.

7. Photoionization efficiency curves for m/e 40 (see text).

8. Time of flight spectra for the indicated mass and laboratory scattering angle. Circles are experimental points, the line is the result of the simulation.

9. Translational energy distribution obtained from the fit to the data in Fig. 8 for the ketene + acetylene channel. The slow contribution to the m/e 26 data that is not fitted arises from secondary decomposition of C_3H_4 (see text).

10. Yield of m/e 39 as a function of laser polarization.

11. Energy diagram (kcal/mol) showing observed products, with barriers obtained from reference 10.

12. Time-of-flight spectra for m/e 28 as a function of probe photon energy near the ionization threshold for CO.
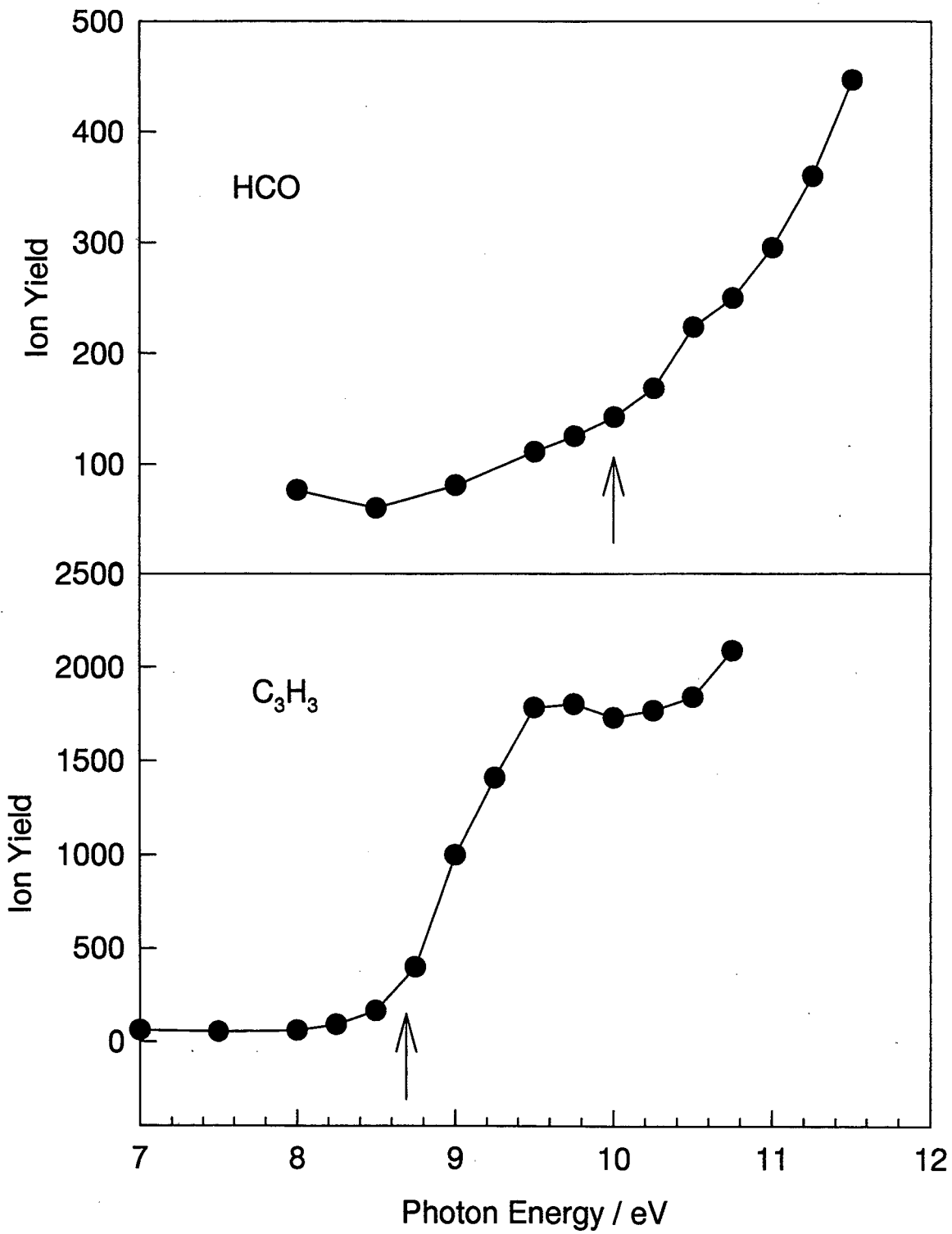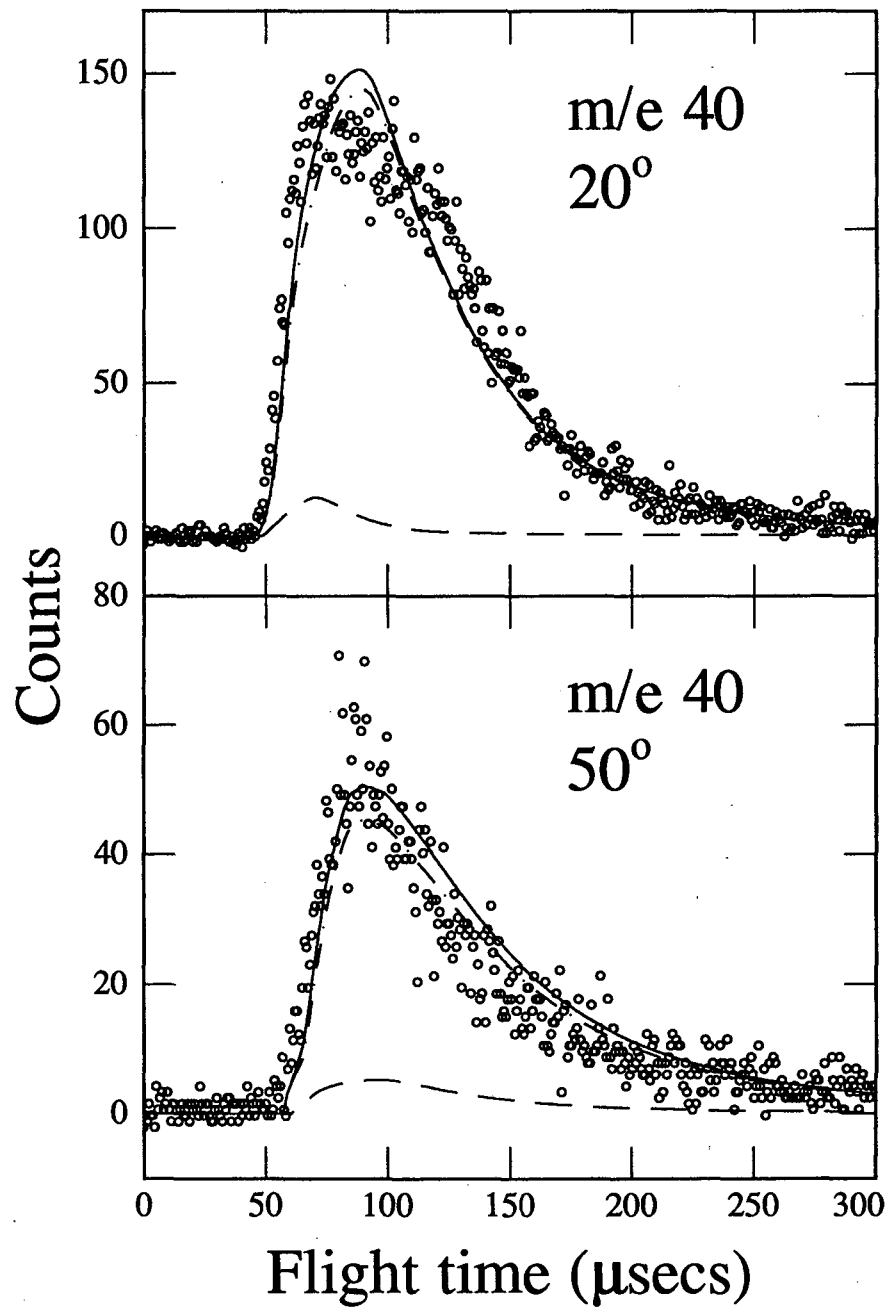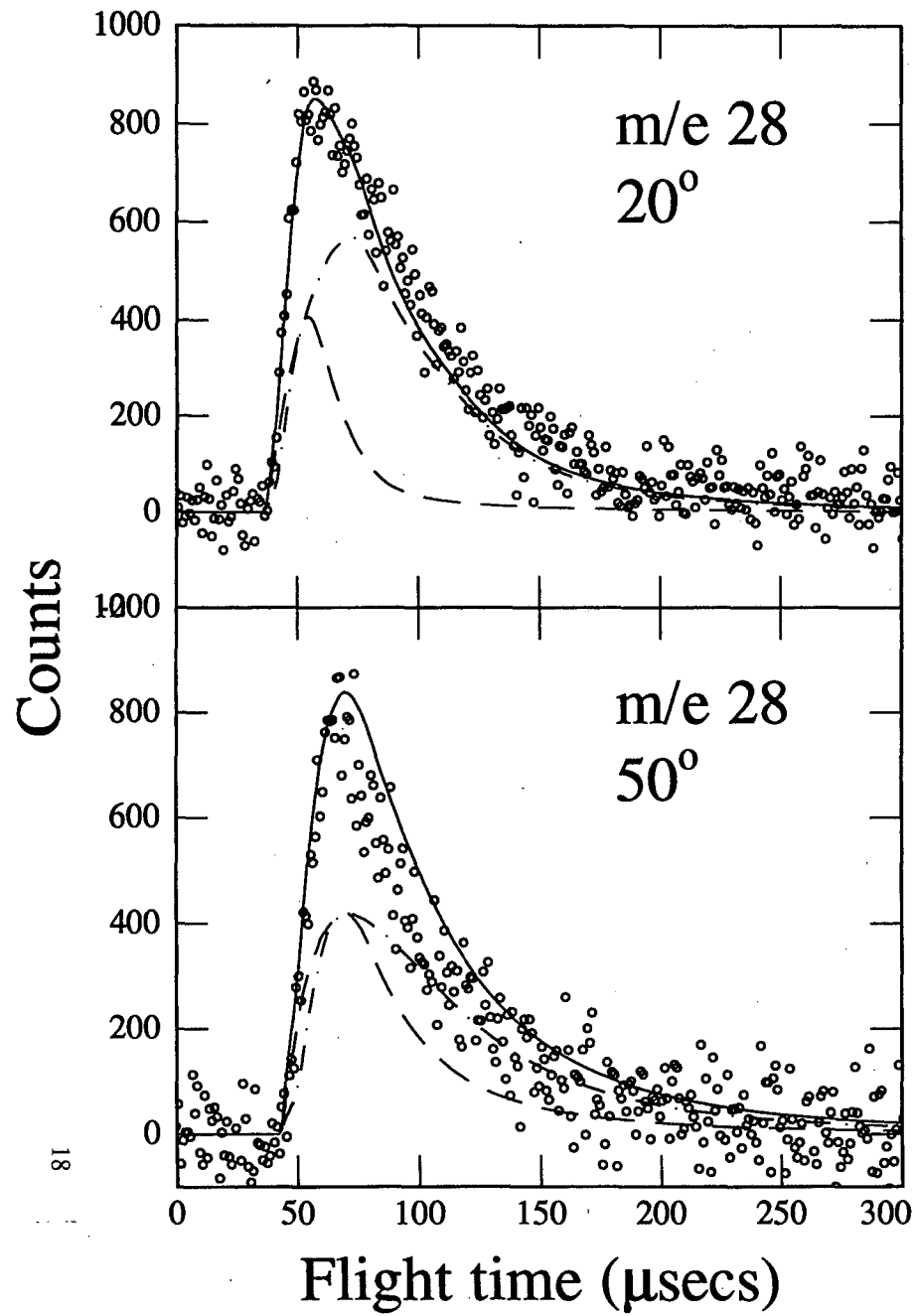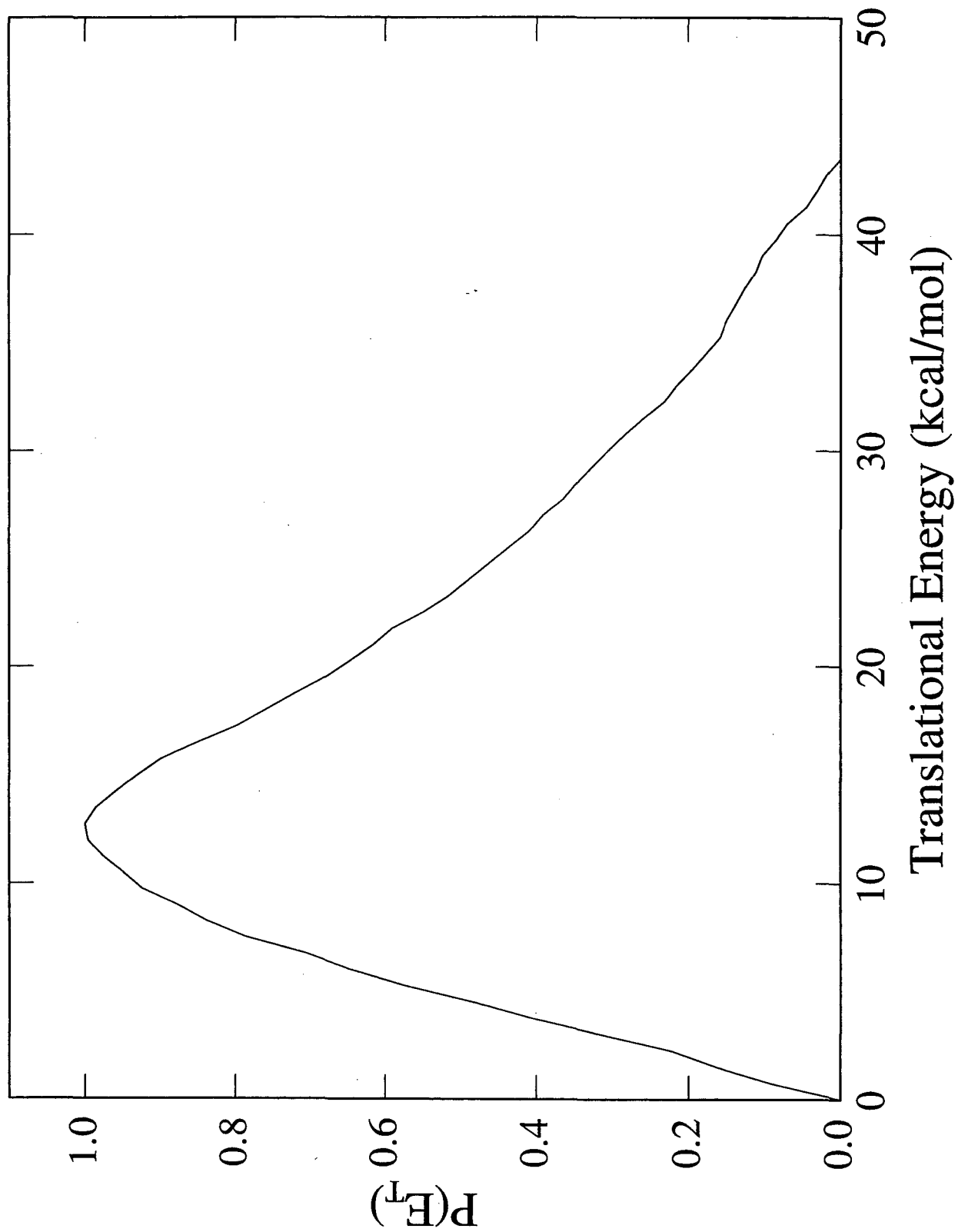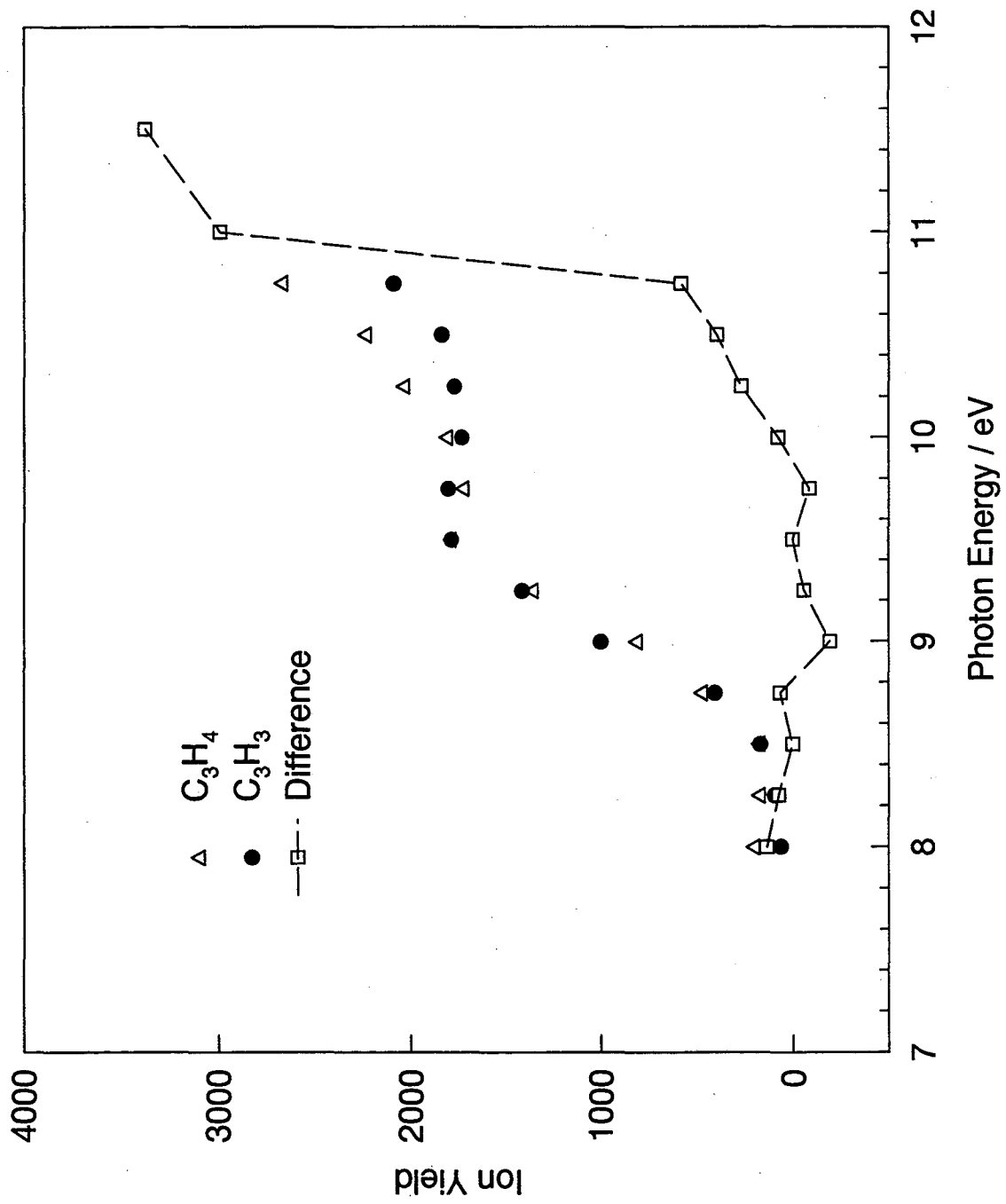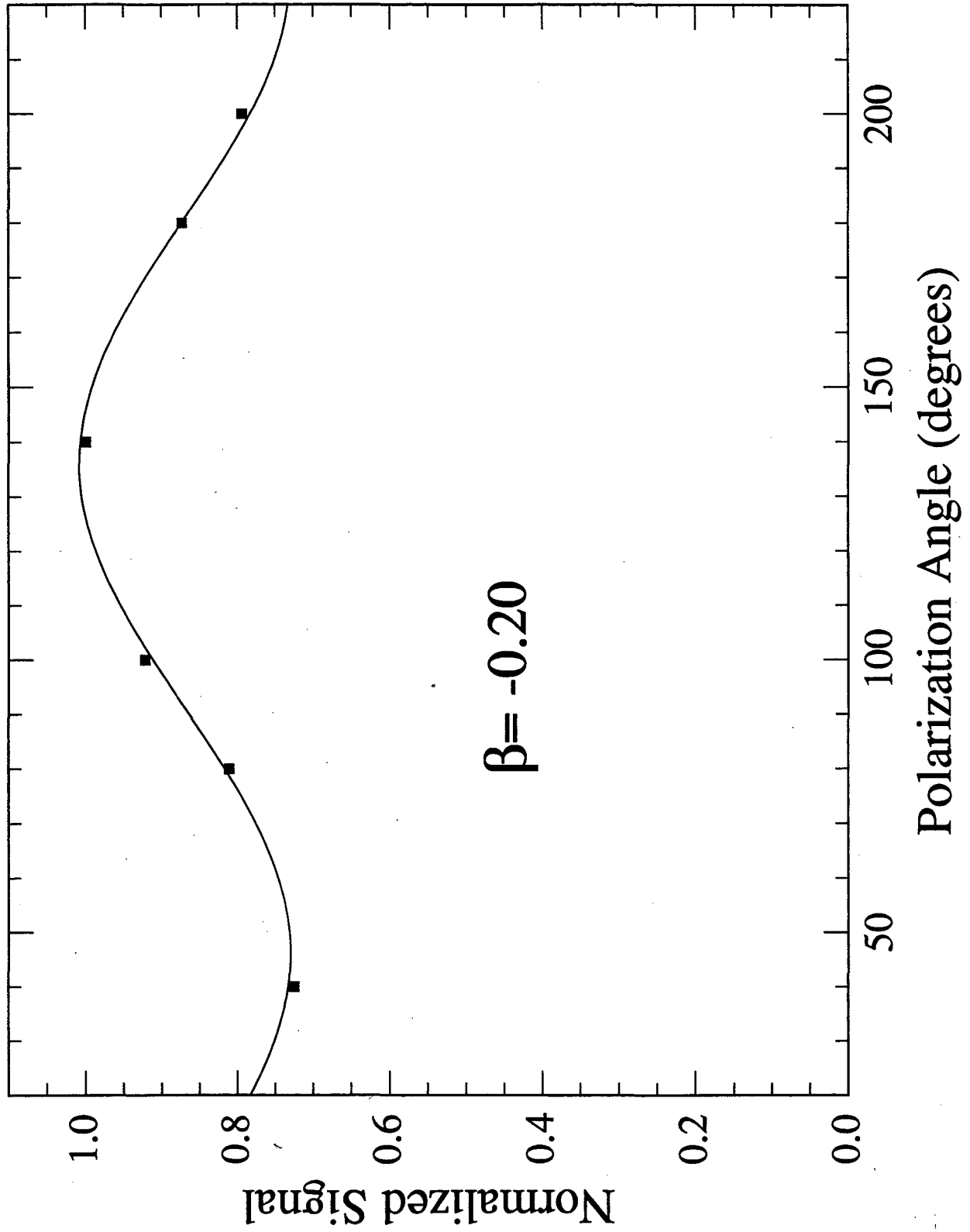
Figure 1

Figure 2

Translational Energy (kcal/mol)

P(E$_T$)

16
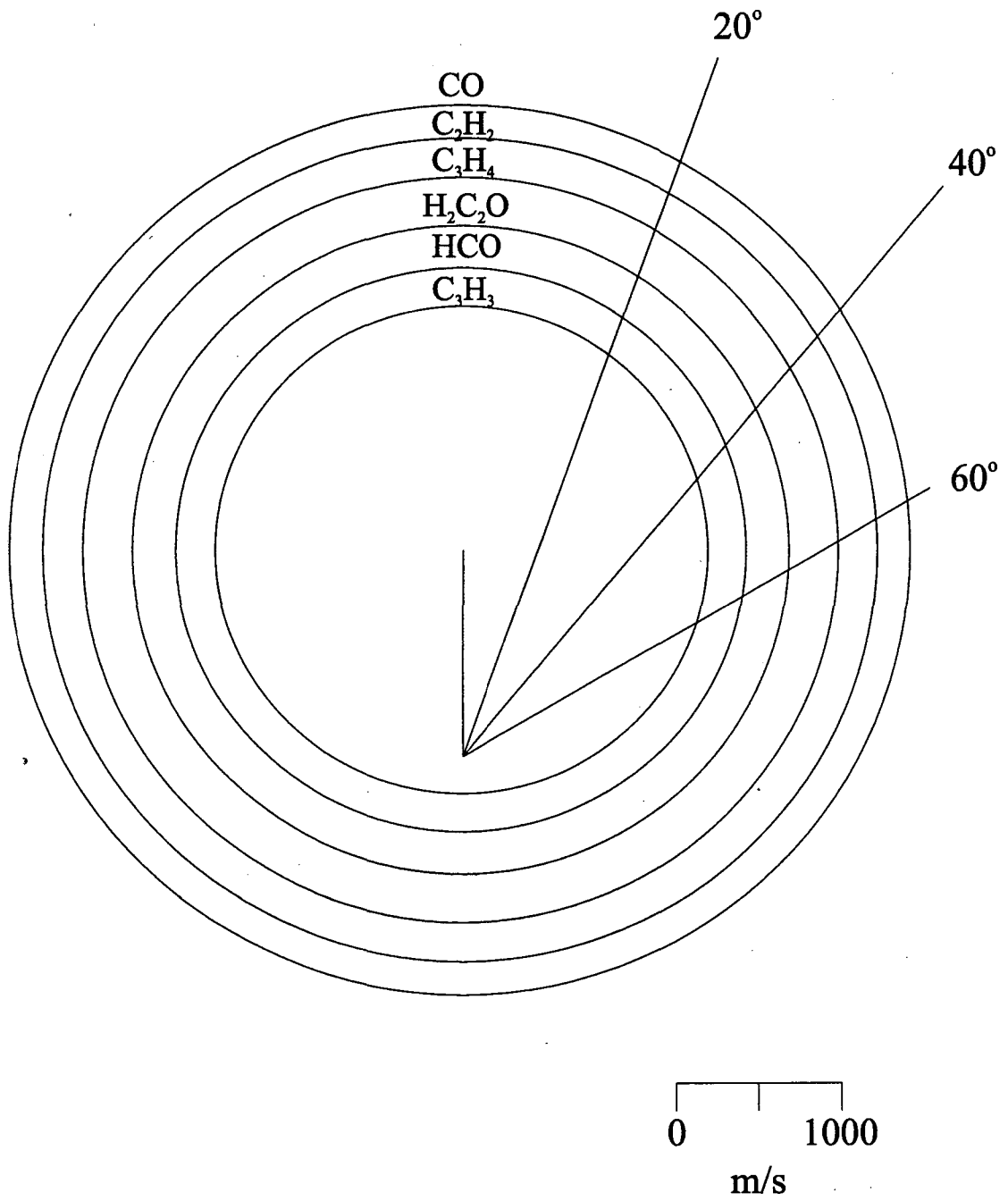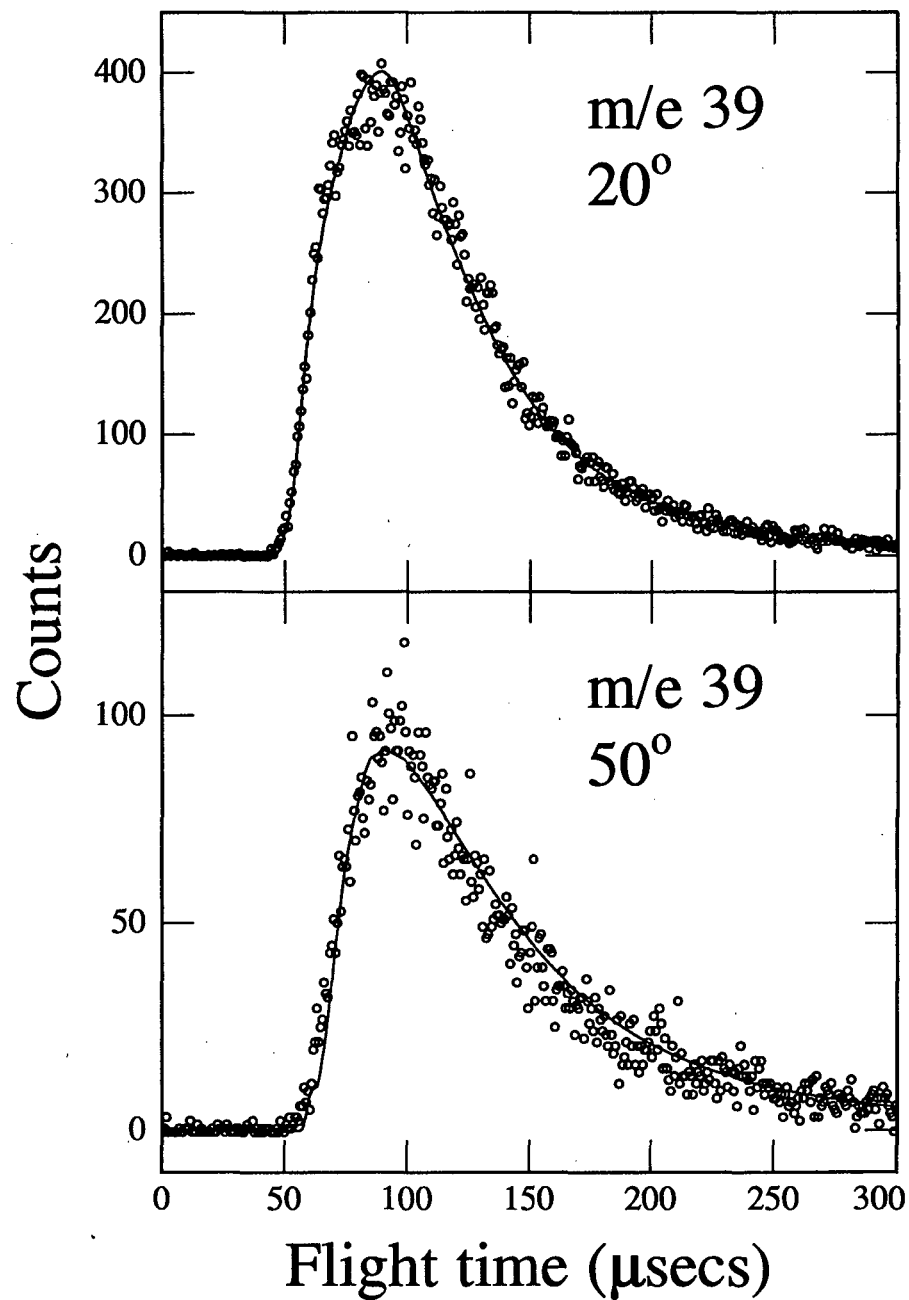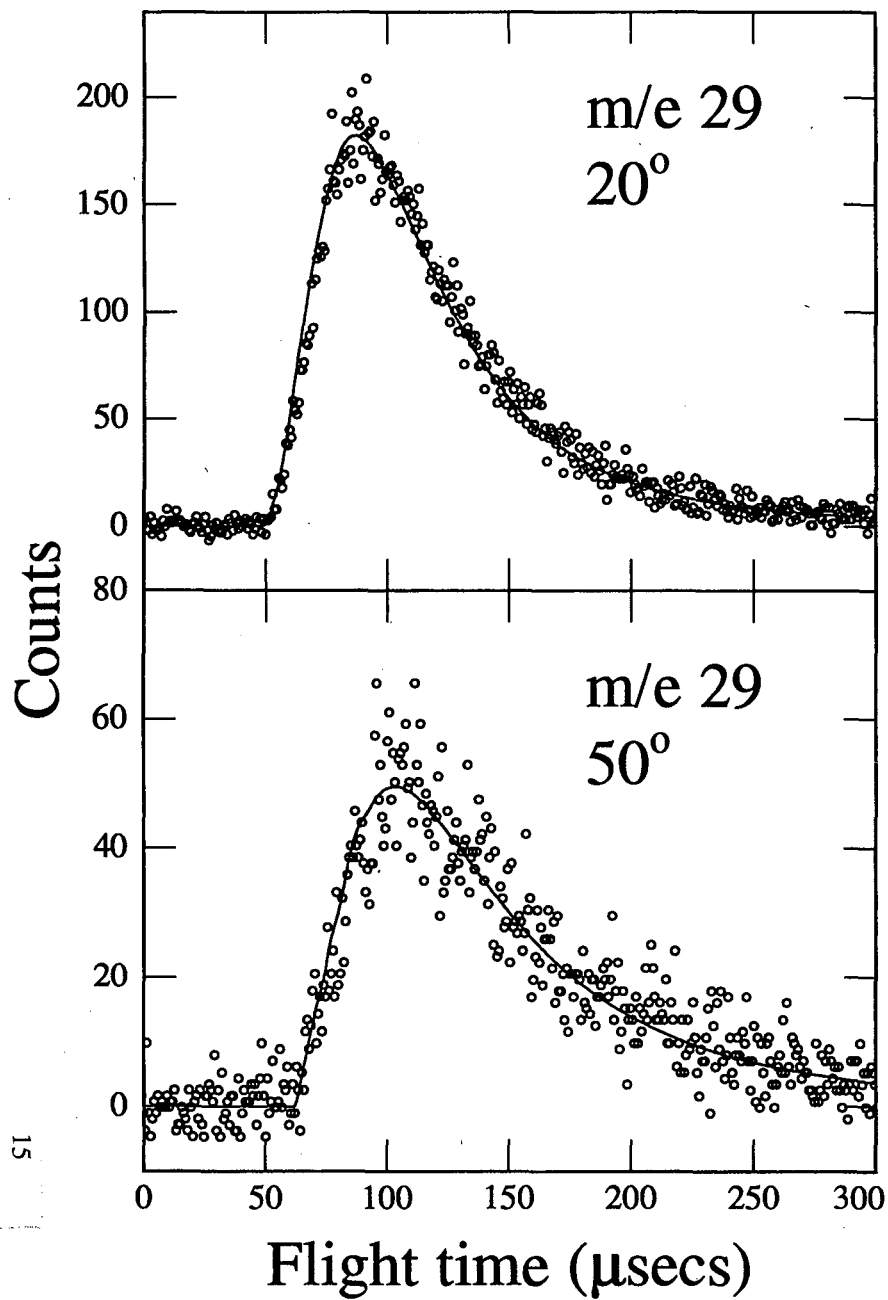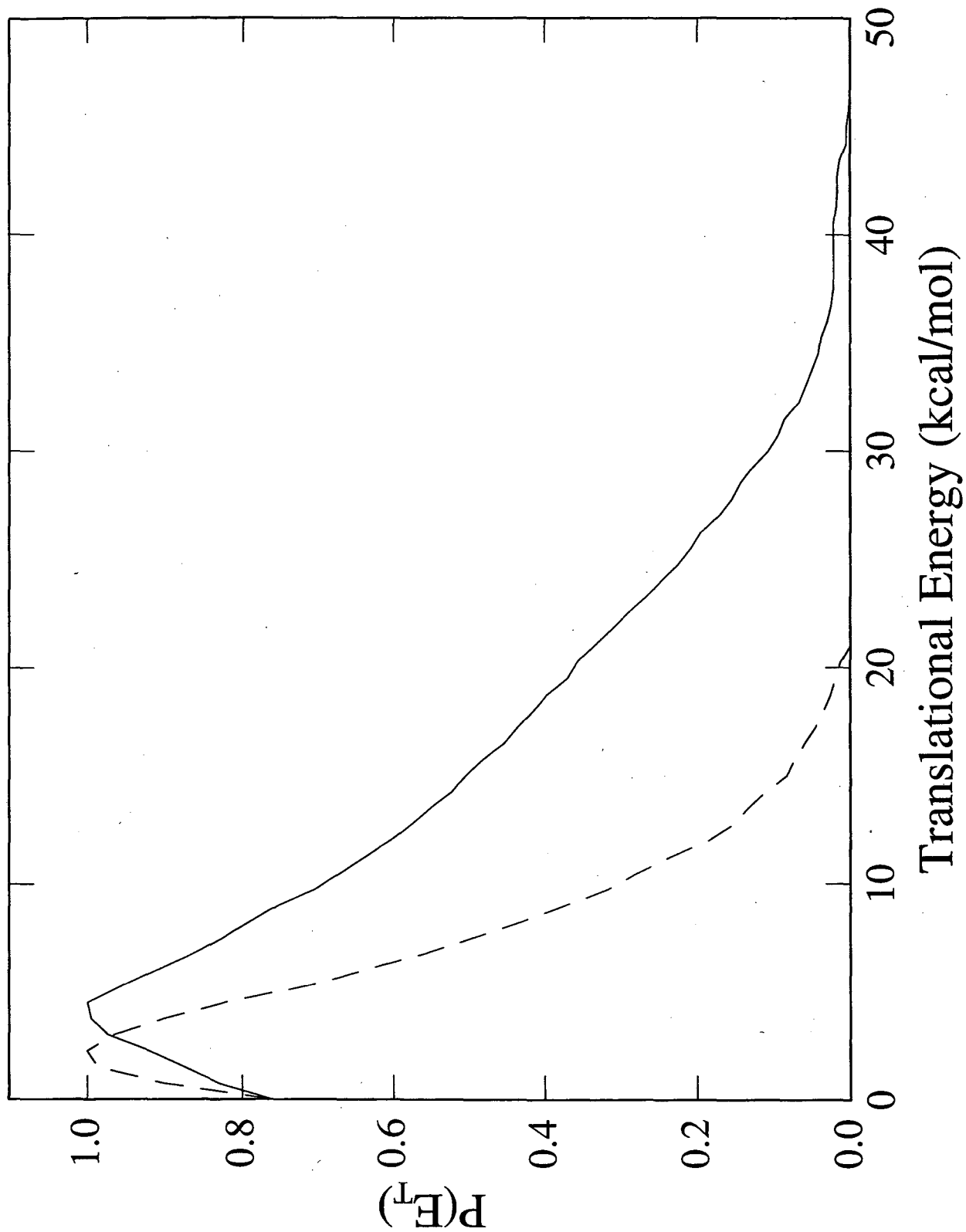
Figure 4

Figure 5

Figure 6

19

Figure 7

20

Figure 8

Figure 9

Figure 10

23

Figure 11

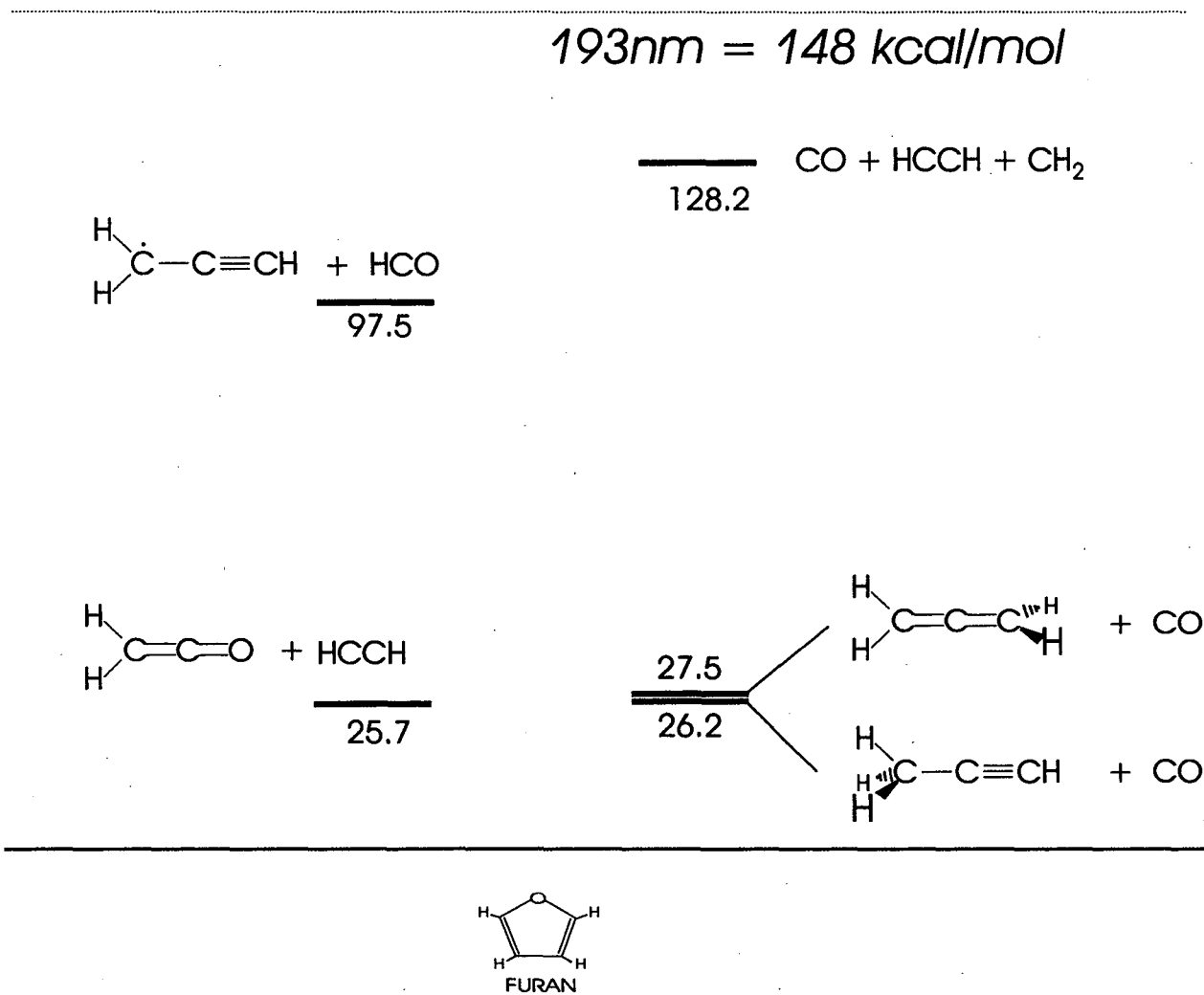hν = 13.46 eV

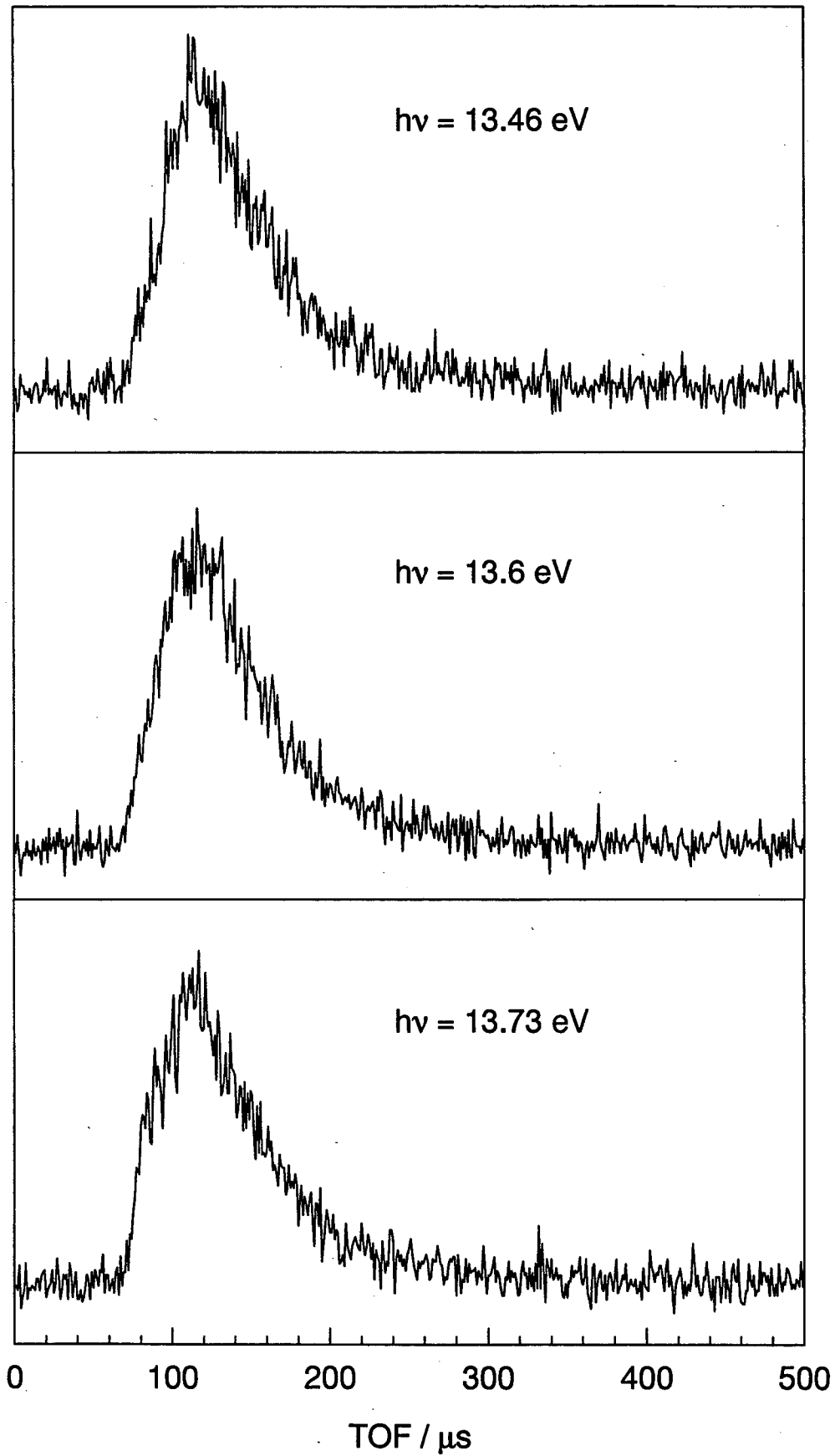hν = 13.6 eV

hν = 13.73 eV

TOF / μs

Figure 12

ERNEST ORLANDO LAWRENCE BERKELEY NATIONAL LABORATORY
ONE CYCLOTRON ROAD ; BERKELEY, CALIFORNIA 94720